PHYSICAL REVIEW B **79**, 220515(R) (2009)

Electron-phonon coupling in compressed 1*T*-TaS_2: Stability and superconductivity from first principles

Amy Y. Liu
Department of Physics, Georgetown University, Washington, DC 20057, USA
(Received 15 March 2009; revised manuscript received 28 April 2009; published 26 June 2009)

The coexistence of charge-density waves and superconductivity in compressed 1*T*-TaS_2 is investigated through density-functional calculations. It has been speculated that this coexistence arises from a real-space phase separation of insulating domains of the commensurate-charge-density-wave phase and metallic interdomain regions. Approximating the structure of the interdomain regions with the undistorted 1*T* structure, the present calculations confirm that pressure suppresses the charge–density-wave instability and stabilizes the interdomain phase. The electron-phonon coupling constants of the compressed 1*T* phase are found to have strong wave-vector dependence, with large contributions from soft modes associated with the incipient charge-density wave instability. The pressure dependence of the coupling parameters is discussed in relation to the measured insensitivity of the superconducting transition temperature to pressure.

DOI: 10.1103/PhysRevB.79.220515 PACS number(s): 74.25.Kc, 74.62.Fj, 71.45.Lr, 63.20.kd

Charge-density-wave (CDW) formation and superconductivity both result from electronic instabilities that lead to collective behavior of electrons in materials. In the well-studied layered dichalcogenides $NbSe_2$ and $TaSe_2$, which undergo both CDW and superconducting transitions, the application of pressure has been found to lower the CDW transition temperature, while increasing the superconducting T_c, suggesting a competition between the two phenomena.[1] On the other hand, the phonon softening associated with CDW formation might be expected to enhance superconductivity as the CDW transition is approached from the undistorted phase.[2]

Recent experiments exploring the pressure-temperature phase diagram of 1*T*-TaS_2 have suggested the possibility of CDW order and superconductivity coexisting not in the same phase, but rather via a phase separation in real space.[3] At ambient pressure, TaS_2 undergoes a series of transitions upon cooling: at about 540 K, the metallic undistorted 1*T* structure (denoted normal or *N*) transforms to an incommensurate (I) CDW phase; at 350 K, the material adopts a nearly commensurate (NC) CDW structure; and below 180 K, a transition to a commensurate (C) CDW phase is observed. The 180 K structural transition is accompanied by an electronic transition that is generally believed to arise from Mott-Hubbard physics.[4] Resistivity measurements indicate that application of less than 1 GPa pressure kills the Mott insulating commensurate CDW, presumably because of changes in bandwidth and screening. The system adopts the non-metallic NC CDW phase between about 1 and 8 GPa, above which the resistivity becomes fully metallic. Between 3–25 GPa, the material exhibits a superconducting transition at low temperatures. The superconducting T_c rises steeply from 0 to about 5 K between 3–5 GPa, then remains roughly constant up to 25 GPa.[3]

The measured superconducting T_c is surprisingly insensitive to the change in the underlying CDW order and to pressure. A mechanism in which the superconducting and CDW phases are separated in real space has been proposed to explain these observations.[3] The NC CDW phase of 1*T*-TaS_2 consists of domains that are locally commensurate with the atomic lattice, separated by interdomain regions.[5,6] It has been conjectured that with pressure, the CDW domains shrink and disappear around 8 GPa.[3] The insensitivity of the superconducting T_c to the suppression of the NC CDW phase could then be explained (at least in part) by superconductivity occurring only in the interdomain regions.

Here we explore the plausibility of this model of CDW and superconducting phases that coexist in TaS_2 due to spatial inhomogeneities in the structure. First-principles density-functional calculations are used to investigate the structural stability of 1*T*-TaS_2 under pressure. We examine the stability of the *N* and C phases directly, and use the *N* phase as an approximation for the interdomain structure in the NC phase. The electron-phonon coupling parameters and the implications for superconductivity in the compressed metallic *N* phase are also investigated.

Calculations were carried out within density-functional theory (DFT) as implemented within the PWSCF code.[7] Ultrasoft pseudopotentials[8] were used to describe the interaction between electrons and ionic cores. For exchange and correlation, the PW91 parametrization of the generalized gradient approximation (GGA) was used.[9] One-electron wave functions were expanded in a plane-wave basis set with a kinetic-energy cutoff of 35 Ry. For structural optimization of the undistorted 1*T* structure, the Brillouin zone was sampled on a uniform mesh of $16\times16\times8$ **k** points, while for the commensurate CDW phase, **k** point meshes of $4\times4\times8$ were used. Phonon spectra and electron-phonon coupling constants were calculated using density-functional perturbation theory.[10] For the undistorted 1*T* structure, a grid of $8\times8\times4$ phonon wave vectors **q** were sampled. Since the frequency and stability of soft phonon modes were found to be very sensitive to the plane-wave cutoff for the charge density, a large cutoff of 1500 Ry was used for the charge density in the phonon calculations. The double Fermi-surface integrals in the definition of the electron-phonon coupling parameters were calculated using the double-tetrahedron method[11] on a grid of $32\times32\times16$ **k** points.

The undistorted 1*T* structure (*N*) is trigonal, with space group $P\bar{3}m1$.[12] It consists of S-Ta-S trilayer units in which atoms in each layer are arranged on a triangular lattice (Fig.

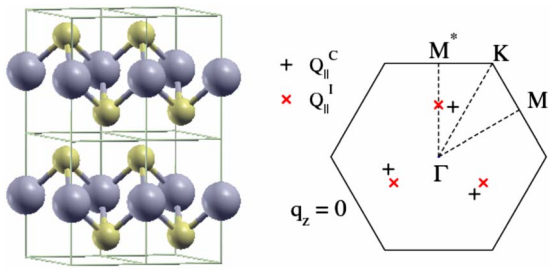

FIG. 1. (Color online) 1*T*-TaS_2 crystal structure and Brillouin zone. The large spheres represent Ta atoms and the small spheres represent S atoms. Since the symmetry of the structure is trigonal, the *M* and M^* points in the Brillouin zone are labeled separately. The in-plane components of the CDW wave vectors for the C and I phases are shown.

1). Since the spacing between trilayer units is large compared to the interlayer spacing within a trilayer unit, the structure is quasi-two-dimensional.

The low-temperature C phase is characterized by a triplet of CDW wave vectors oriented at 120° with respect to each other, yielding a $\sqrt{13}\times\sqrt{13}$ supercell within the basal plane.[13] The 13 Ta atoms in each supercell condense into a star-of-David cluster, accompanied by a buckling of the neighboring S planes. The projection of the CDW wave vector on the basal plane $\mathbf{Q}_\parallel^C$ has magnitude $2\pi/\sqrt{13}a$ and is rotated by 13.9° from the primitive reciprocal lattice vector of the undistorted phase, as shown in Fig. 1. The stacking of the trilayer units in the C CDW phase is likely disordered.[14]

The NC CDW phase consists of domains made up of the C CDW star-of-David clusters separated by interdomain regions with reduced displacement amplitudes.[5,6] In the out-of-plane direction, the stacking sequence repeats after three trilayer units. Detailed structural information about the interdomain regions, particularly under pressure, is not available.

The structure of the I CDW phase at ambient pressure is characterized by a triplet of wave vectors with $\mathbf{Q}_\parallel^I=\mathbf{b}/\sqrt{13}$, where **b** is an in-plane primitive reciprocal lattice vector of the *N* phase (Fig. 1). The CDW amplitude is smaller in the I phase than in the C phase.[15]

Since pressure generally suppresses CDW formation due to a stiffening of the lattice, in this work we use the undistorted *N* structure to approximate both the compressed metallic phase and the interdomain regions in the phase that evolves from the zero-pressure NC phase.

The phonon dispersion curves for the *N* phase at ambient pressure are plotted as dotted lines in Fig. 2. The dispersion is very two dimensional, as evidenced by the flatness of the curves in the Γ to *A* direction.[16] In fact, the in-plane dispersion curves look nearly identical for all values of q_z. One of the acoustic branches is dynamically unstable about half way along the high-symmetry Γ to M^* line. The location of this instability, which persists for all q_z, coincides closely with the projections of both the I and C CDW wave vectors in the basal plane. There are also anomalies in the acoustic branches along the Γ to *K* direction, but these branches remain stable. The eigenvectors of the unstable modes involve atomic displacements that are primarily in plane for Ta atoms and out of plane for S atoms, consistent with the observed

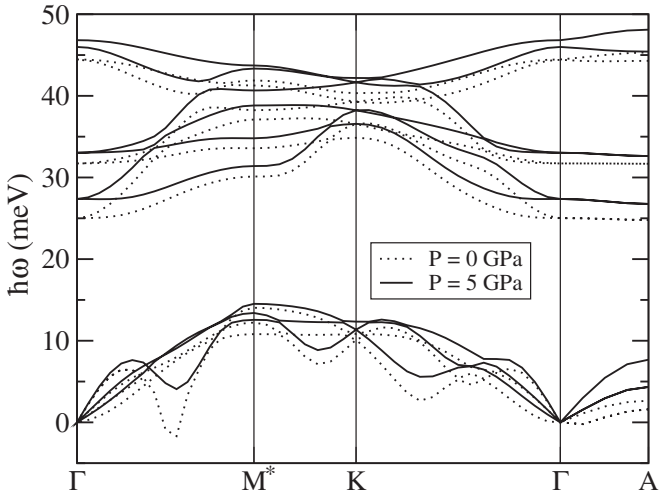

FIG. 2. Calculated phonon dispersion curves for 1*T*-TaS_2 at $P=0$ and 5 GPa. Imaginary frequencies, corresponding to unstable modes, are represented as negative frequencies.

CDW distortions. The calculated insensitivity of these modes to q_z is consistent with a disordered stacking of trilayer units in the *c* direction, as observed in the C CDW phase.

Between 0 and 5 GPa, the calculated in-plane lattice parameter *a* contracts by about 1.5%, while the out-of-plane *c* drops over 9%. Most of the change in the *c* direction is absorbed by the intertrilayer separation. As shown in Fig. 2, this leads to a significant hardening of the modes that correspond to nearly rigid displacements of trilayer S-Ta-S units, i.e., the acoustic modes along Γ-*A*. The structure also becomes dynamically stable. With increasing pressure, the phonon spectrum hardens, but even at 30 GPa (not shown), anomalies in the acoustic branches along the Γ to M^* and Γ to *K* directions persist, signaling the incipient CDW instability.

To further examine the lattice instability, we have done total-energy calculations for a $\sqrt{13}\times\sqrt{13}\times1$ supercell that corresponds to the C CDW supercell in the basal plane but assumes simple stacking out of the plane. Structures were relaxed from configurations in which the Ta atoms were displaced off their high-symmetry *N* sites while maintaining the symmetry of the experimentally determined C CDW structure. Thus the energy landscape was probed within the subspace consistent with the experimentally determined C CDW structure.

At zero pressure, a small radial displacement of Ta atoms off the high-symmetry sites of the undistorted 1*T* structure causes the system to relax into a structure with star-of-David clusters in which the first ring of Ta atoms contracts inwards by 6% and the second ring contracts inwards by 4%. These atomic displacements, as well as those of the S atoms, which bulge outwards near the center of the Ta clusters, are similar to structures determined from x-ray diffraction.[13] At 5 GPa, the calculations find a reduced amplitude for the CDW (2% and 1% for the first and second Ta rings, respectively). In addition, the energy surface has a local minimum corresponding to the undistorted *N* phase, consistent with the dynamic stability of the *N* structure found in the linear-response calculations. The energy difference between the C and *N*

TABLE I. Calculated electronic, vibrational, and superconducting properties of 1*T*-TaS_2. The pressure P is in GPa, the electronic density of states at the Fermi level $N(E_F)$ is in states/Ry/spin, the characteristic phonon energies are in meV, and the superconducting T_c is in K.

P	$N(E_F)$	$\hbar\omega_{av}$	$\hbar\omega_{log}$	λ	T_c
5	10.6	28.3	5.9	2.09	16.0
10	9.1	29.9	9.1	1.23	10.0
20	7.9	32.6	13.7	0.82	7.2
30	7.4	34.2	16.9	0.69	5.9

phases is too small to resolve in our calculations. At 10 GPa, Ta atoms displaced from the high-symmetry sites relax back to the N structure, and no C CDW minimum is found in the energy surface.

While we are not able to directly model the textured NC and the I phases and our calculations do not include the strong correlation physics of the C phase, we can still comment on aspects of the structural phase diagram. At ambient pressure, our $T=0$ DFT results show that the balance of electronic and elastic energies favors a CDW distortion at both $\mathbf{Q}^I$ and $\mathbf{Q}^C$. In the C phase, there is presumably an addition lowering of the electronic energy due to the opening of a Mott-Hubbard gap, making it more favorable than the I phase at low temperatures. On the other hand, the multitude of soft modes in the undistorted N structure give large contributions to the phonon entropy, making it the favored structure at high temperatures. With pressure, the CDW amplitude decreases because the elastic energy cost of the distortion grows. With this reduction in CDW amplitude and the decrease in lattice constant, the overlap between orbitals on neighboring star-of-David clusters is enhanced, which tends to suppress the Mott transition. By 5 GPa, the DFT energies for the N phase and C phase (with reduced amplitude) are approximately equal. A uniform C phase at this pressure is not fully gapped by either electron-electron interactions or the CDW distortion, but given the near degeneracy of the homogeneous N and C phases, it is plausible that a charge transfer from CDW domains to metallic interdomain regions could be energetically favorable, as proposed in Ref. 3. Alternatively, a nonuniform distribution of stress, in which the stress is lower in the C domains than in the interdomain regions, could help stabilize the textured phase by allowing the C CDW domains to remain gapped.

For pressures at which the N structure is calculated to be stable (i.e., $P \geq 5$ GPa), we have investigated the electron-phonon coupling constant λ, which is related to both superconductivity and the CDW instability. Starting from high pressures, far from the CDW instability, a moderate coupling constant of $\lambda=0.69$ is found at 30 GPa. With decreasing pressure, as the system approaches the CDW instability, λ grows, reaching 2.09 at 5 GPa (Table I). The λ-weighted characteristic frequency ω_{log} is much smaller than the average frequency, especially at low pressures, indicating large contributions to the coupling from low-frequency modes. Furthermore, the coupling is very nonuniform across the Brillouin zone. Figure 3(a) shows the wave-vector-dependent

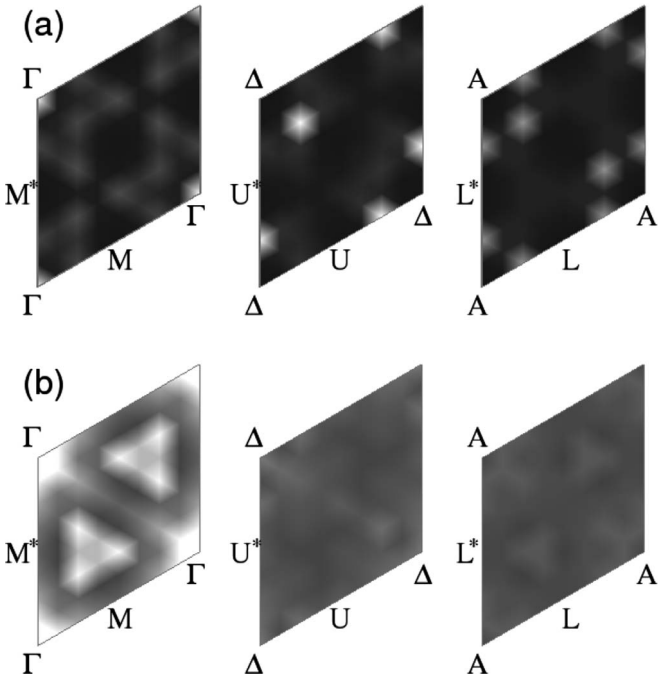

FIG. 3. Calculated (a) electron-phonon coupling parameters and (b) nesting function for 1*T*-TaS_2 at 5 GPa. From left to right, the panels correspond to $q_z=0, \pi/2c$, and π/c. The linear gray scales use white to represent a large value and black to indicate a small value.

$\lambda_{\mathbf{q}}$, at $P=5$ GPa. On the linear gray scale used in the figure, large values of $\lambda_{\mathbf{q}}$ show up as white. The largest contributions come from soft modes with wave vectors that have in-plane components close to $\mathbf{Q}_{\parallel}^I$ and $\mathbf{Q}_{\parallel}^C$.

Fermi-surface nesting has been proposed as a driving mechanism for the CDW transition in 1*T*-TaS_2 at ambient pressure.[17] The existence of a broad but weak local maximum in the nesting function at $\mathbf{Q}^I$, along with significant overlap of the nested areas of the N Fermi surface with Brillouin-zone boundaries of the I superstructure, have been interpreted as evidence for an electronic origin for the I CDW instability.[18] On the other hand, more recent photoemission data have revealed features that are not compatible with a simple Peierls scenario.[19] To probe the role that nesting plays in the CDW instability, we have calculated the nesting function, which is related to the imaginary part of the noninteracting susceptibility, as a function of pressure. Figure 3(b) shows the nesting function at 5 GPa. Comparison of panels (a) and (b) in Fig. 3 shows there is little correlation between the $\mathbf{q}$ dependence of the electron-phonon coupling and that of the nesting function. Corresponding plots for 0 and 10 GPa look qualitatively similar. Over this range of pressures, the strongest nesting clearly occurs away from the CDW wave vectors, while the largest contributions to λ come from the modes that become unstable at the CDW transition. Hence the CDW instability has its origins in strong electron-lattice coupling rather than in a purely electronic mechanism. The irrelevancy of geometric nesting of the Fermi surface to the CDW instability in another transition metal dichalcogenide, $NbSe_2$, has been discussed recently in Ref. 20.

Within the Migdal-Eliashberg theory of strong-coupling superconductivity, the superconducting transition temperature T_c depends on the electron-phonon spectral function $\alpha^2F(\omega)$ and the screened Coulomb parameter μ^*. The spectral function measures the effectiveness of phonons of energy $\hbar\omega$ to scatter electrons from one part of the Fermi surface to another, and its inverse-frequency moment is proportional to the coupling constant λ. Using the calculated α^2F and assuming $\mu^*=0.14$, which is typical for transition-metal compounds, we have solved the Eliashberg equations to find the transition temperatures listed in Table I. The value of the calculated T_c is within a few K of the measured T_c at high pressures, which is considered good agreement for this type of calculation. However, the calculated pressure dependence appears to be incompatible with the nearly constant T_c observed in experiments.

This discrepancy, which is significant at low pressures, could be due in part to an inhomogeneous distribution of stress in the textured phase. If the pressure within the interdomain regions is actually higher than the applied pressure, the observed T_c at low pressures would be smaller than the calculated values. As the C domains shrink, the pressure in the interdomain regions would approach the applied pressure. While it has been hypothesized that the C domains disappear around 8 GPa based on the metallic nature of the resistivity,[3] the data do not preclude the continued existence of C CDW domains to higher pressures. Overall, the dependence of T_c on the applied pressure would then be weaker than the results presented in Table I. The discrepancy between the measured and calculated $T_c(P)$ could also be due to the assumptions we have made about the structure of the metallic regions. Approximating the interdomain structure as *N* like is probably least accurate at low pressures, where the interfaces with the C CDW domains can have a significant impact.

We have shown that the electron-phonon interaction plays an important role in CDW formation in TaS_2 and that it can also account for the magnitude of the observed superconducting T_c at high pressures. The observed lack of pressure dependence in T_c remains a puzzle. Further experimental and theoretical investigations into the structure of $1T$-TaS_2 under compression are needed to better address the nature of the superconducting state in this material.

I thank Jim Freericks, Yizhi Ge, and Igor Mazin for helpful discussions. This research was supported by the NSF through Grant No. DMR-0705266 and through TeraGrid resources provided by TACC and NCSA.

[1] C. Berthier, P. Molinie, and D. Jerome, Solid State Commun. **18**, 1393 (1976).
[2] E. G. Maksimov, in *High-Temperature Superconductivity*, edited by V. L. Ginzburg and D. A. Kirzhnits (Consultants Bureau, New York, 1982), Chap. 4.
[3] B. Sipos, A. F. Kusmartseva, A. Akrap, H. Berger, L. Forro, and E. Tutis, Nature Mater. **7**, 960 (2008).
[4] P. Fazekas and E. Tosatti, Philos. Mag. B **39**, 229 (1979).
[5] R. E. Thomson, B. Burk, A. Zettl, and J. Clarke, Phys. Rev. B **49**, 16899 (1994).
[6] A. Spijkerman, J. L. de Boer, A. Meetsma, G. A. Wiegers, and S. van Smaalen, Phys. Rev. B **56**, 13757 (1997).
[7] http://www.pwscf.org
[8] D. Vanderbilt, Phys. Rev. B **41**, 7892 (1990).
[9] J. P. Perdew, J. A. Chevary, S. H. Vosko, K. A. Jackson, M. R. Pederson, D. J. Singh, and C. Fiolhais, Phys. Rev. B **46**, 6671 (1992).
[10] S. Baroni, S. de Gironcoli, A. Dal Corso, and P. Giannozi, Rev. Mod. Phys. **73**, 515 (2001).
[11] I. I. Mazin and A. Y. Liu (unpublished).
[12] F. Jellinek, J. Less-Common Met. **4**, 9 (1962).
[13] R. Brouwer and F. Jellinek, Physica B & C **99**, 51 (1980).
[14] S. Tanda, T. Sambongi, T. Tani, and S. Tanaka, J. Phys. Soc. Jpn. **53**, 476 (1984).
[15] L. D. Chapman and R. Colella, Phys. Rev. B **32**, 2233 (1985).
[16] At ambient pressure, the GGA underestimates the weak binding between trilayer units, so the two-dimensional nature of the phonon dispersion curves is likely exaggerated.
[17] J. A. Wilson, F. J. Di Salvo, and J. Mahajan, Adv. Phys. **24**, 117 (1975); H. W. Myron and A. J. Freeman, Phys. Rev. B **11**, 2735 (1975); A. M. Woolley and G. Wexler, J. Phys. C **10**, 2601 (1977).
[18] M. Bovet, D. Popovic, F. Clerc, C. Koitzsch, U. Probst, E. Bucher, H. Berger, D. Naumovic, and P. Aebi, Phys. Rev. B **69**, 125117 (2004).
[19] F. Clerc, C. Battaglia, M. Bovet, L. Despont, C. Monney, H. Cercellier, M. G. Garnier, P. Aebi, H. Berger, and L. Forro, Phys. Rev. B **74**, 155114 (2006).
[20] M. D. Johannes, I. I. Mazin, and C. A. Howells, Phys. Rev. B **73**, 205102 (2006).